

RSC Advances



This is an *Accepted Manuscript*, which has been through the Royal Society of Chemistry peer review process and has been accepted for publication.

Accepted Manuscripts are published online shortly after acceptance, before technical editing, formatting and proof reading. Using this free service, authors can make their results available to the community, in citable form, before we publish the edited article. This *Accepted Manuscript* will be replaced by the edited, formatted and paginated article as soon as this is available.

You can find more information about *Accepted Manuscripts* in the [Information for Authors](#).

Please note that technical editing may introduce minor changes to the text and/or graphics, which may alter content. The journal's standard [Terms & Conditions](#) and the [Ethical guidelines](#) still apply. In no event shall the Royal Society of Chemistry be held responsible for any errors or omissions in this *Accepted Manuscript* or any consequences arising from the use of any information it contains.

Effect of graphene nanosheets and layered double hydroxides on the flame retardancy and thermal degradation of epoxy resin

Shan Liu^{1,2}, Hongqiang Yan², Zhengping Fang^{1,2*}, Zhenghong Guo², Hao Wang³

¹ MOE Key Laboratory of Macromolecular Synthesis and Functionalization, Institute of Polymer Composites, Zhejiang University, Hangzhou 310027, China

² Laboratory of Polymer Materials and Engineering, Ningbo Institute of Technology, Zhejiang University, Ningbo 315100, China

³ Centre of Excellence in Engineered Fiber Composites, University of Southern Queensland, Toowoomba, Queensland 4350, Australia

Corresponding authors. Tel./fax: +86 571 87953712. E-mail address: zpfang@zju.edu.cn (Zhengping Fang)

Abstract:

The effects of graphene nanosheets (GNS) and layered double hydroxides (LDH) on morphology, flame retardancy and thermal degradation of epoxy resin (ER) were investigated. LDH was exfoliated in ER/GNS/LDH nanocomposites, while GNS was partially exfoliated and partially agglomerated into small clusters. Since not all of the GNS was in good dispersion, the compactness and barrier properties of residual char in ER/GNS/LDH were inferior to ER/GNS and ER/LDH. However, the simultaneous addition of GNS and LDH created additional GNS-LDH interface, which could increase interaction in the melt and inhibit the flammable drips of ER and thus limit the flame propagation during combustion. As a result, a synergistic effect of simultaneous addition of GNS and LDH to improve the flame retardancy of ER was realized. The LOI value of ER was increased from 15.9 to 23.6 by adding 0.5 wt% of GNS and 0.5 wt% of LDH. In comparison, the LOI value was 19.5 and 21.7 when GNS or LDH was added separately, at the same level, 1 wt%. Furthermore, both GNS and LDH can increase the thermal stability of ER, there was a synergistic effect between them to decrease the THR of ER from 33.4 to 24.6.

Key words: graphene nanosheets, layered double hydroxides, nanocomposite, thermal stability, flame retardancy

1. Introduction

Epoxy resin (ER) is one of the most important thermoset polymers. Owing to its outstanding mechanical stiffness and toughness, good solvent and chemical resistance, and superior adhesion, ER is widely used as a coating, adhesive, laminate, semiconductor encapsulate, and matrix for advanced fiber-reinforced composites. However, cured epoxy resin has high flammability which may affect its application [1-8]. Many approaches have been exploited to

improve the flame retardancy of ER. Nano-sized fillers have recently drawn great interest due to their potential to improve the flame retardancy of pristine polymers at small amount of addition [1, 2, 9, 10].

Graphene nanosheet (GNS) is a new class of nano-sized filler with exceptional functions, high mechanical strength (1 TPa in Young's modulus and 130 GPa in ultimate strength) and chemical stability. Graphene is a single-atom-thick two-dimensional carbon layer, and has triggered considerable interest in developing various of novel composites due to its high surface area, electrical conductivity, high flexibility and mechanical strength. It has exhibited great promise for potential applications in the fields of nanoelectronics, sensors, batteries, super-capacitors, hydrogen storage and nanocomposites [3, 8, 11-12]. GNS is not a single graphene sheet but comprises multiple graphene sheets that are stacked together. Y. Q. Guo investigated the flame retardant properties of graphene, graphite oxide and functionalized graphite oxides in epoxy composites [4]. Micro combustion calorimetry measurements illustrate that graphene composites perform better than graphite oxide composites. The TG-IR indicates graphene sample can promote combustion at low temperature but reduce the gas released at high temperature, which may be due to the layered effect that enhances the flame retardancy and promotes the char formation [4]. In our previous work, in order to increase flame retardant properties of epoxy resin, GNS is added into ER and shows good thermal stability. GNS changed the decomposition pathway of ER at high temperature. The compactness of char residues were significantly improved. Moreover, GNS can effectively decrease melt flow and inhibit the flammable drips of ER. Incorporation of 3 wt% of GNS increased the LOI value of ER from 15.7 to 21.0 and reduced the total heat release from 33.37 to 28.20 kJ/m² [5].

Layered double hydroxides (LDH), a class of 2D nano-structured anionic clays whose structure is based on brucite (Mg(OH)₂)-like layers, can be easily synthesized on a large scale. Most metals, such as Fe, Co, Ni, Cu, Zn, Mg, Al, Ca and Li, can be arranged at an atomic level in a lamellar of LDH flake with controllable components. This is attributed to the substitution of divalent metal cations by trivalent cations within their hydroxide-like layers, which leads the LDH layer to be positively charged and balanced by a wide variety of anions within their interlayer domains [13-19]. Some studies on LDH address their potential use as non-halogenated, non-toxic flame-retardant nano-filler for polymers [2, 14-17]. It is reported that LDH contribute to the flame retardancy of the polymeric matrix, producing a refractory oxide residue on the surface of the material and releasing aqueous vapor and carbon dioxide during decomposition. The endothermic nature of these processes and the dilution of combustible gases of pyrolysis increase the ignition time and reduce the heat release during combustion [1].

Flammability of polymer is assessed primarily through ignitability, flame spread, and heat release [1]. We speculate that the simultaneous additions of GNS and LDH can increase the flame retardancy of ER. GNS can reduce

the gas released at high temperature, promote the char formation and enhance the barrier properties [3]. LDH can increase the ignition time at low temperature and reduce the heat release during combustion [1]. If we combine these two nano-fillers effectively, the flame retardancy of matrix will be greatly improved both at high temperature and low temperature during combustion.

So far the effect of GNS/LDH to increase flame retardant property of thermoset polymer has not been studied systematically. This paper aims to synthesize Mg-Al LDH and prepare the ER/GNS/LDH nanocomposites, evaluate the influence of GNS and LDH on the morphology, thermal stability and flame retardancy of ER. The mechanism the flame retardancy in ER/GNS/LDH during combustion has also been discussed.

2. Experimental

2.1 Materials

Epoxy resin (JY-256, density 1.13-1.15 g/cm³, epoxy value 0.54-0.56 mol/100g) was obtained from Jiafa Chemical Co. Ltd., Changshu, China. Poly (propylene glycol) bis (2-aminopropyl) ether (Jeffamine D230, Huntsman Co., Houston Texas, America.) were used as curing agents. Graphene nanosheets (JCGNP-1) with an average density of 2.25 g/cm³ and a purity of >99.5% was obtained from Jcnano Technology Co. Ltd., Nanjing, China. Al(NO₃)₃·9H₂O and Mg(NO₃)₂·6H₂O (analytical pure) were supplied by China National Pharmaceutical Group Corporation (Sinopharm). NaOH (analytical pure) were obtained from Shanghai Chemical Reagents Co., China.

2.2 Preparation of LDH

The LDH was prepared by the co-precipitation method previously described by Miyata [8]. A solution of Mg(NO₃)₂·6H₂O (0.1 mol) and Al(NO₃)₃·9H₂O (0.05 mol) was slowly added into 150 mL of decarbonated water under N₂ atmosphere at a constant pH = 10.0 adjusted by simultaneously drop-wise addition of a 0.5 mol NaOH aqueous solution. The prepared solution was heated to 100°C under continuous magnetic stirring for 12 h in a flask (equipped with a reflux condenser) of 500 mL under ambient atmosphere. Then, the obtained suspension was kept at 95°C for another 12 h without stirring. After filtering, washing and freeze-drying, the final products were Mg/Al-LDH. Figure 1 is the SEM images of GNS (a) and LDH (b). SEM pictures showed that the thickness of GNS and LDH flakes were at nano-scale. The width of LDH flakes (about 50~70 nm) was smaller than GNS flakes. The size of LDH flakes was almost uniform.

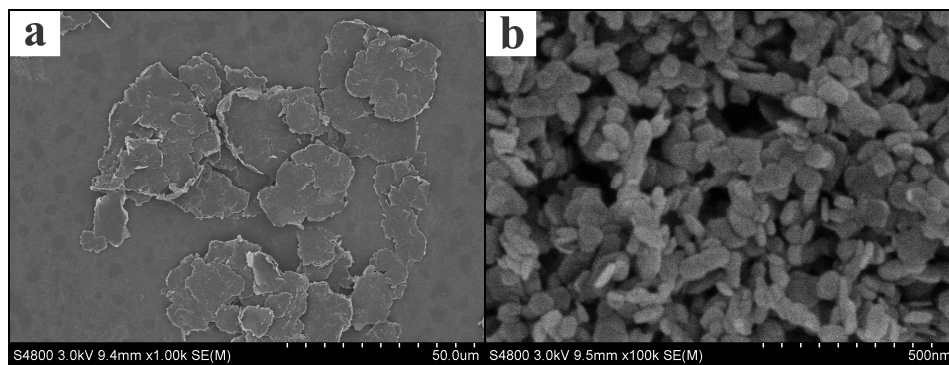


Figure 1. SEM images of (a) GNS and (b) LDH.

2.3 Preparation of ER/GNS, ER/LDH and ER/GNS/LDH composites

An appropriate content of GNS was dispersed in acetone (100 mL of acetone to 0.01 g of GNS) with ice bath, ultrasonicated and stirred for 1.5 h. The epoxy monomer was added to the mixture and ultrasonicated for another 1.5 h. To remove the acetone, the solution was put into 70°C oil bath and stirred for 5 h, then transferred to a vacuum chamber at 70°C for 1 h to remove the residual acetone. Subsequently, the mixture was cooled to 25°C then curing agent was added with stirring for 0.5 h. The mixture was again placed in a vacuum chamber to degas for 1 h, then carefully poured into silicone rubber moulds with injector, pre-cured at 50°C for 5 h, and post-cured at 110°C for 2 h to obtain the ER/GNS composite samples. The ER/LDH samples were prepared by the same procedure while the solvent was replaced by N, N-Dimethylformamide (DMF) and the evaporation temperature was 160°C. The samples were identified as ER/GNS x (mass ratio of ER/GNS = 100/ x) and ER/LDH y (mass ratio of ER/LDH = 100/ y), respectively.

To prepare ER/GNS/LDH composites, same procedure was followed. An appropriate content of GNS and LDH was dispersed in acetone and DMF respectively with ice bath. After the epoxy monomer was added, acetone and DMF were removed by putting the solution into a 160°C oil bath. The pre-cured and post-cured samples were identified as ER/GNS x /LDH y (mass ratio of ER/GNS/LDH = 100/ x/y).

2.4 Characterization

A Hitachi S-4800 (Hitachi, Japan) scanning electron microscope (SEM) was used to observe the micro-morphology of composites. The samples were coated with a gold layer about 10 nm in thickness to improve the conductivity of the surface. X-ray diffraction (XRD) was carried out to determine the interlayer distances of GNS and LDH. All tests were conducted by using a Rigaku X-ray generator (Cu K α radiation) in the reflection mode at

room temperature. Transmission electron micrograph (TEM) images were obtained on a JEM-1200EX electron microscope (JEM, Japan) with an accelerating voltage of 120 kV. The sample of about 70 nm in thickness was ultrathin-sectioned with a diamond knife. Limiting oxygen index (LOI) was measured by using an HC-2 Oxygen Index Instrument (Jiangning Analyser Instrument, China) on sheets ($100 \times 6 \times 3 \text{ mm}^3$) according to ASTM D2863-2008. Micro combustion calorimetry (MCC) was performed on a Govmak MCC-2 Microscale Combustion Calorimeter (Govmak, USA). The incident heat flux was 45 kW/m^2 and about 5 mg samples were heated to 700°C at a heating rate of 1°C/s and in a stream of nitrogen flowing at $80 \text{ cm}^3/\text{min}$. Each test was repeated three times. Thermogravimetric analysis/infrared spectrometry (TG-IR) was carried out using a TGA 209 F1 thermal analyzer (NETZSCH, Germany) interfaced to a Thermo Nicolet iS10 FTIR spectrophotometer (Nicolet). Samples were heated to 700°C at a heating rate of $20^\circ\text{C}/\text{min}$, and each specimen was examined in triplicate. The accuracy temperature and mass measurement were $\pm 1^\circ\text{C}$ and $\pm 0.1 \text{ wt}\%$.

3. Results and Discussion

3.1 Structure and morphology

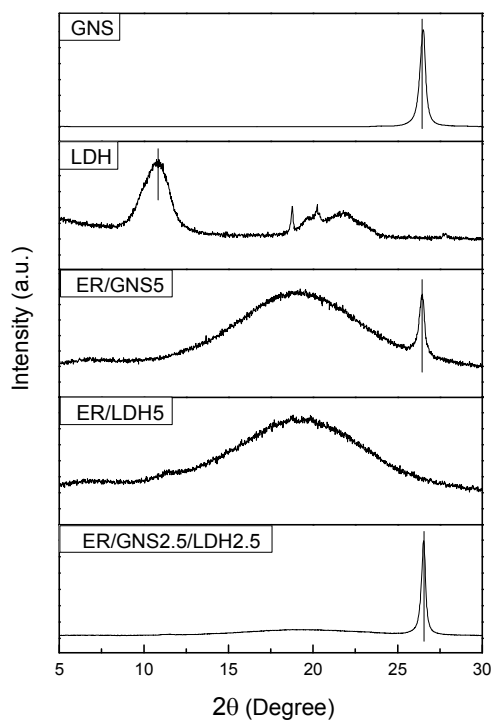


Figure 2. XRD patterns of GNS, LDH, ER/GNS5, ER/LDH5 and ER/GNS2.5/LDH2.5 composites.

XRD patterns of GNS, LDH, ER/GNS, ER/LDH and ER/GNS/LDH composites were shown in Figure 2. In GNS, the sharp diffraction peak of 2θ at 26.5° featured an interlayer spacing of 0.34 nm. The diffraction peak of GNS still existed in ER/GNS composites without shifting. The restacking and agglomeration of GNS occurred in ER/GNS composites. The diffraction peak of 2θ at 10.9° in LDH featured an interlayer spacing of 0.81 nm, which was larger than GNS. There was no obvious diffraction peak of LDH in ER/LDH composite, revealing all LDH was exfoliated in ER/LDH composites. In ER/GNS/LDH composites, the diffraction peak of GNS still existed, the diffraction peak of LDH disappeared. This result indicated that LDH was exfoliated while some GNS was agglomerated in ER/GNS/LDH composites.

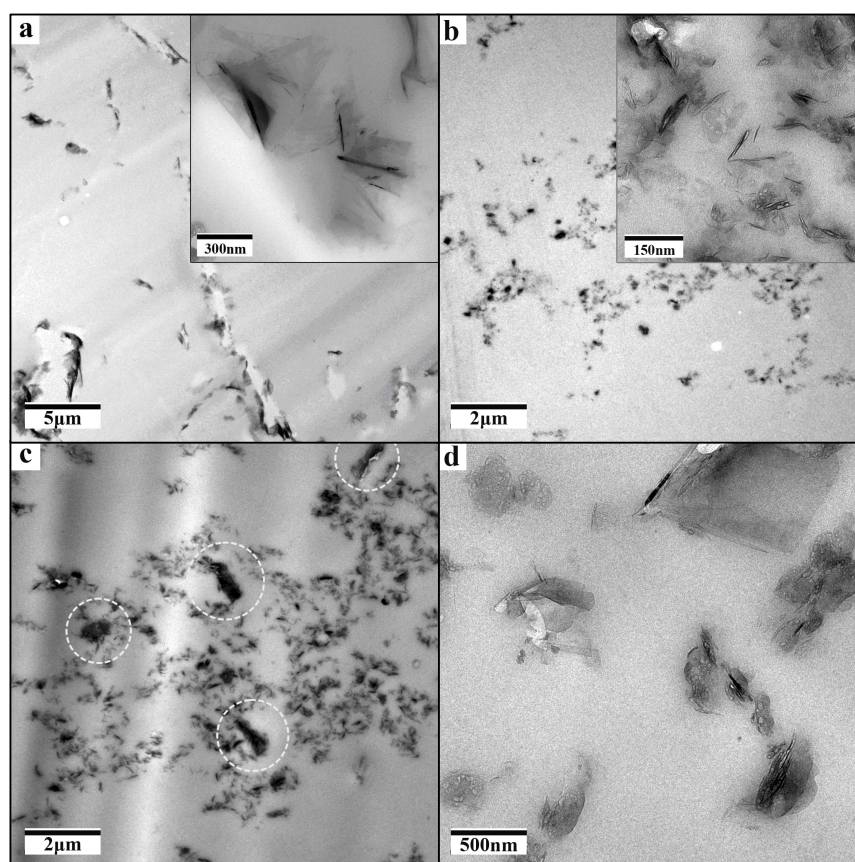


Figure 3. TEM images of (a) ER/GNS5, (b) ER/LDH5, (c, d) ER/GNS2.5/LDH2.5 under different magnifications.

To determine the dispersion of GNS and LDH, TEM analysis was carried out. Figure 3 (a, b) were the TEM images of ER/GNS5 and ER/LDH5 respectively. The small pictures in the top right corner were their corresponding images at a high magnification. Figure 3 (c, d) were the TEM images of ER/GNS2.5/LDH2.5 with different magnifications.

In ER/GNS5, there were some GNS agglomerations. Some large and flat graphene flakes can be seen under high magnification. The size of GNS flakes were about 300~500 nm. In ER/LDH5, the distribution of LDH was substantially uniform. We can see that LDH are single-layered under high magnification. LDH flakes were about 50~100 nm. All LDH exfoliated in ER/LDH5 nanocomposites. In ER/GNS2.5/LDH2.5 composites, some small clusters (in the white dashed circles) were observed under low magnification. The clusters were found consisting of agglomerated GNS. Other small layers with good dispersion were the homogeneous mixture of LDH and GNS which can be seen under high magnification in Figure 3d. The dispersion of GNS in ER/GNS and LDH in ER/LDH was similar as they were in ER/GNS/LDH. The exfoliated GNS and agglomerated GNS coexisted in ER/GNS/LDH nanocomposites. All LDH exfoliated in ER/GNS/LDH nanocomposites.

3.2 Thermal degradation and flame retardant properties

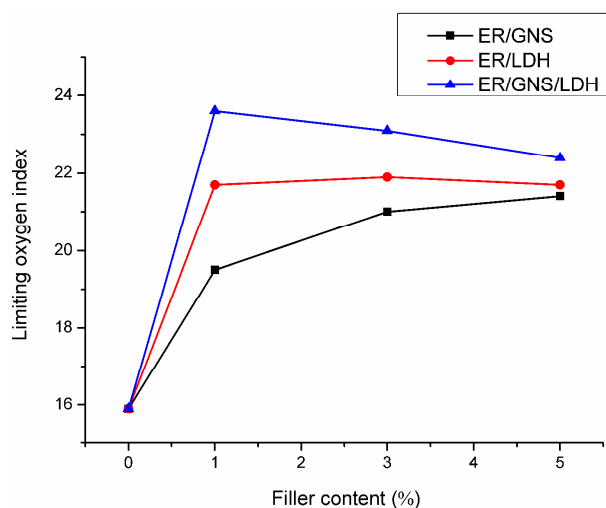


Figure 4. LOI of ER, ER/GNS, ER/LDH and ER/GNS/LDH composites with different filler content.

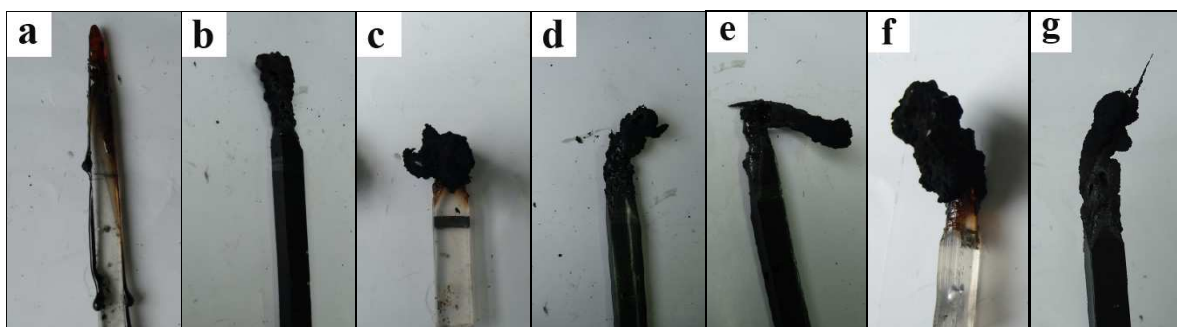


Figure 5. The patterns of samples after LOI tests: (a) ER, (b) ER/GNS1, (c) ER/LDH1, (d) ER/GNS0.5/LDH0.5, (e) ER/GNS5, (f) ER/LDH5, (g) ER/GNS2.5/LDH2.5.

By definition, synergism effect means enhanced performance of the mixture of two or more components compared to the simple additive performance of the components at the same concentration [1]. To verify whether there is a synergistic effect between GNS and LDH to improve the flame retardancy of ER, we selected three groups (ER/GNS1, ER/LDH1, ER/GNS0.5/LDH0.5; ER/GNS3, ER/LDH3, ER/GNS1.5/LDH1.5 and ER/GNS5, ER/LDH5, ER/GNS2.5/LDH2.5) for comparison.

LOI data of ER, ER/GNS, ER/LDH and ER/GNS/LDH composites were shown in Figure 4. The LOI value of ER was 15.9, indicated its inherent flammability. For ER/GNS systems, the LOI value increased with the increase of GNS content, the increase became less significant after 3% addition. For ER/LDH systems, the addition of 1 wt% of LDH increased the LOI value of ER effectively, but the LOI value can not be further improved with the increase of LDH content. For ER/GNS/LDH systems, there was a synergistic effect between GNS and LDH to improve the LOI value of ER. The LOI value was increased to 23.6 at the addition of 0.5 wt% GNS and 0.5 wt% LDH together, which is higher than addition of GNS (19.5) or LDH (21.7) alone at the same addition level, 1 wt%.

The patterns of samples after LOI tests were shown in Figure 5. The patterns of pure ER sample in LOI test had some melt dripping while the ER/GNS, ER/LDH and ER/GNS/LDH composites had not during combustion. The reason was that: In ER, some flexible chains existed in macromolecular network which apt to break in high temperature. There was a tendency to spread flame away from a fire source, so the LOI value of ER was low. GNS was in the form of layers, which can play the role of barrier and effectively increase the viscosity, decreasing the melt flow [20, 21]. The incorporation of the LDH nano-particles restrained the relative motion of the polymer chain and made the nano-composites “stiffer” [22]. An attractive polymer-matrix interface (GNS-ER in ER/GNS) and (LDH-ER in ER/LDH) inhibited the movement of ER segments during combustion and thus tended to inhibit the flammable drips of ER. The simultaneous addition of GNS and LDH to ER matrix made the system have additional GNS-LDH interactions compared to ER/GNS and ER/LDH, which could further increased the viscosity of the melt, limited flame propagation through the inhibition of dripping. Hence, there was a synergistic effect between GNS and LDH to improve the LOI value of ER.

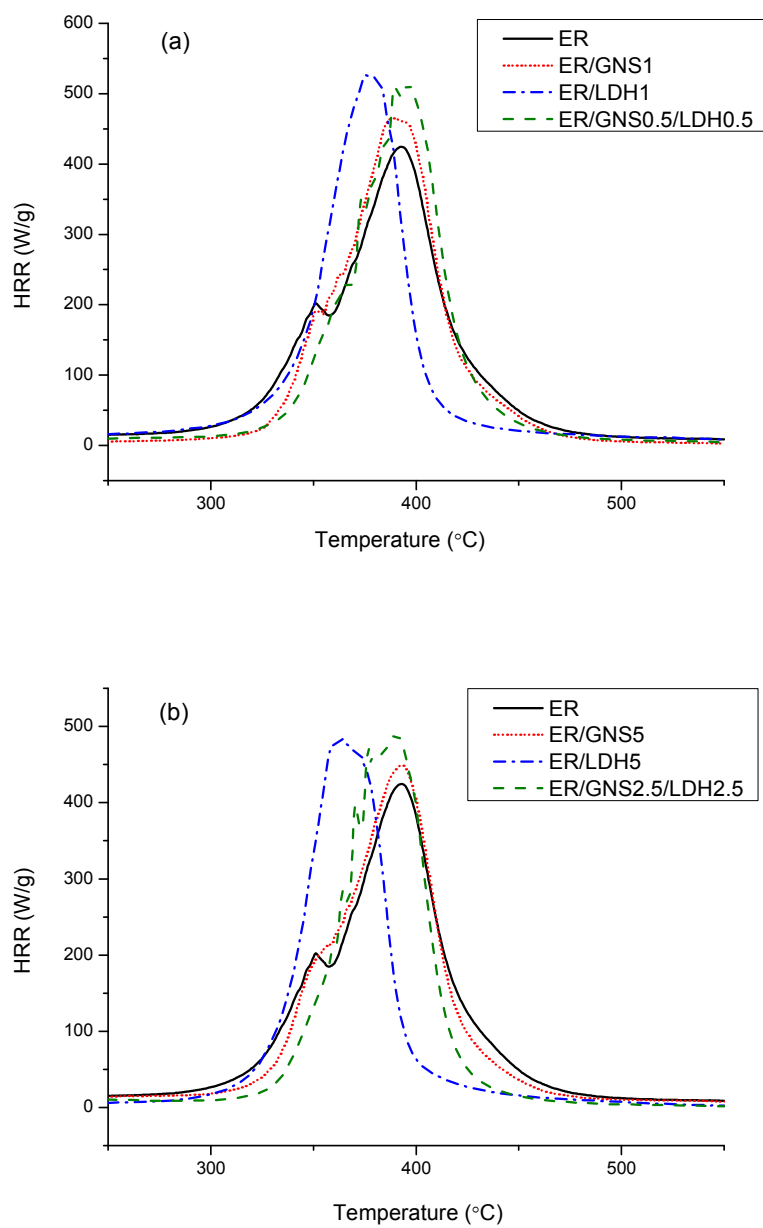


Figure 6. MCC curves of ER, ER/GNS, ER/LDH and ER/GNS/LDH composites.

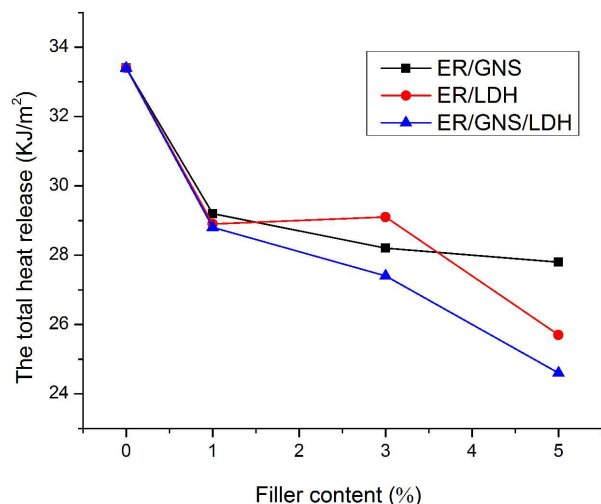


Figure 7. THR of ER, ER/GNS, ER/LDH and ER/GNS/LDH composites with different filler content.

MCC curves of ER, ER/GNS, ER/LDH and ER/GNS/LDH were showed in Figure 6. The Total Heat Released (THR) data were shown in Figure 7. From Figure 6 and Figure 7 we can see that, the THR of ER composites decreased with the addition of GNS and LDH compared to pure ER. When added GNS and LDH together, the THR of ER/GNS/LDH were much lower than the pure ER, ER/GNS and ER/LDH composites. There was a synergistic effect between GNS and LDH to decrease the THR of ER. The THR value of ER was decreased from 33.4 to 24.6 at the addition of 2.5 wt% GNS and 2.5 wt% LDH together, which is lower than addition of GNS (27.8) or LDH (25.7) alone at the same addition level, 5 wt%. Peak Heat Release Rate (PHRR) of ER composite increased with the addition of GNS, which was studied in our previous research [5]. PHRR of ER/LDH and ER/GNS/LDH increased while the temperature of the maximum heat release (T_{max}) of them decreased compared to pure ER, this is due to the huge amount of aqueous vapor generated by LDH in combustion.

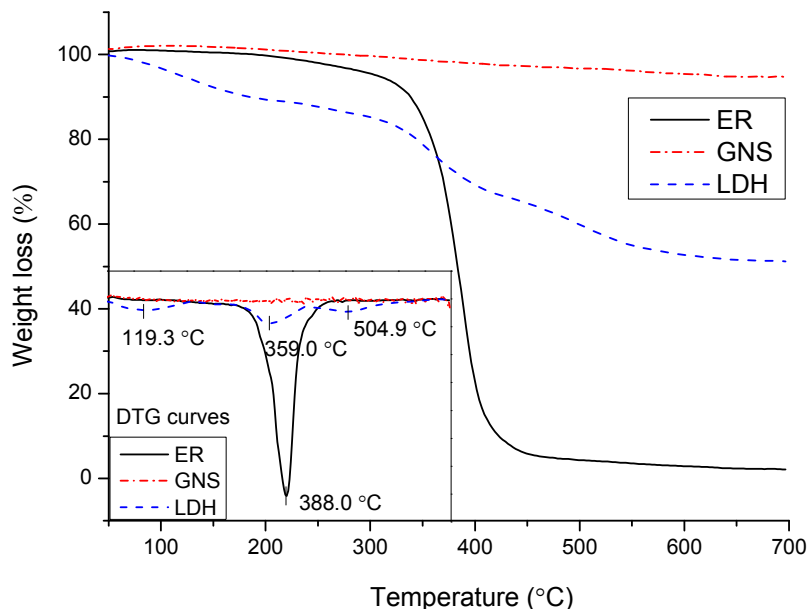


Figure 8. TG and DTG curves of ER, GNS and LDH under nitrogen atmosphere.

Figure 8 were the TG curves of ER, GNS and LDH under nitrogen atmosphere. The T_{\max} of samples were obtained from its derivative. In the thermal degradation of ER main chains, the cross-linked polyaromatic carbonaceous residue formed, involved elimination of water through dehydration of secondary alcohol groups and the formation of unsaturated structures. Further degradation of precursor char and small molecular gaseous species occurred with the increase of temperature. A small amount of char residue (≈ 2.1 wt%) was observed at 700°C. During the degradation of ER, there was a strong DTG peak at 388.0°C (T_{\max}). In GNS there was only a small amount of decomposition, the char residue at 700°C achieved 95.8 wt%. The decomposition of LDH was a three-step process. At low temperature, the decomposition corresponded to the loss of interlayer water, then the condensation of hydroxyls of the octahedral layer, together with decomposition of the anion NO_3^{2-} at higher temperatures. The decomposition was strongly endothermic. The residues (≈ 51.2 wt%) was composed of magnesium oxide and aluminum oxide. During the degradation process of LDH, there was three stage of weight loss corresponding to DTG peaks at 119.3°C, 359.0°C and 504.9°C. Below the onset degradation temperature of ER, the GNS did not begin to decomposition, but LDH began to decomposition and to release non-flammable gases (water vapor and carbon dioxide).

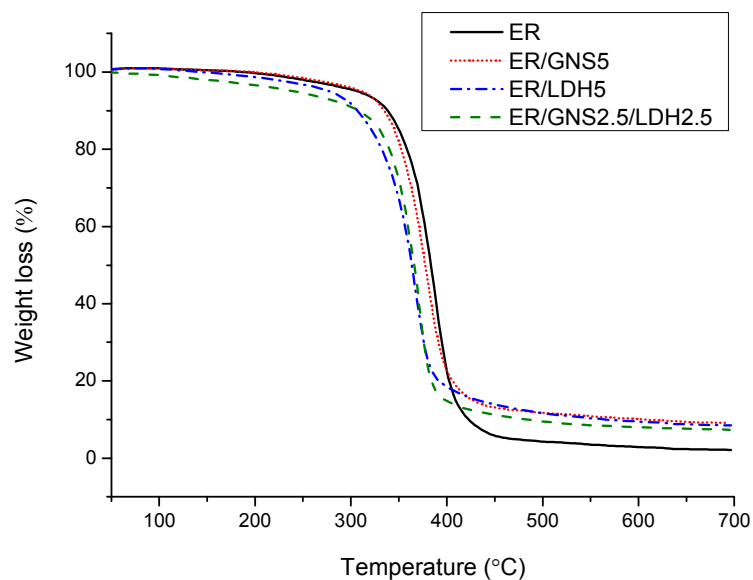
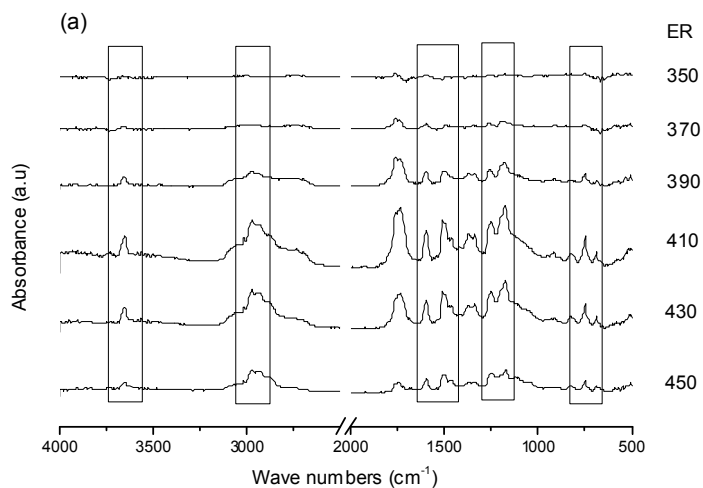


Figure 9. TG curves of ER, ER/GNS5, ER/LDH5 and ER/GNS2.5/LDH2.5 composites under nitrogen.

Table 1. TG and DTG data under nitrogen atmosphere.

Sample	$T_{-5\%}$ (°C)	T_{max} (°C)	Char residue (%)
ER	306.8	388.0	2.1
ER/GNS5	311.0	378.9	9.0
ER/LDH5	276.8	366.9	8.4
ER/GNS2.5/LDH2.5	240.3	371.0	7.3



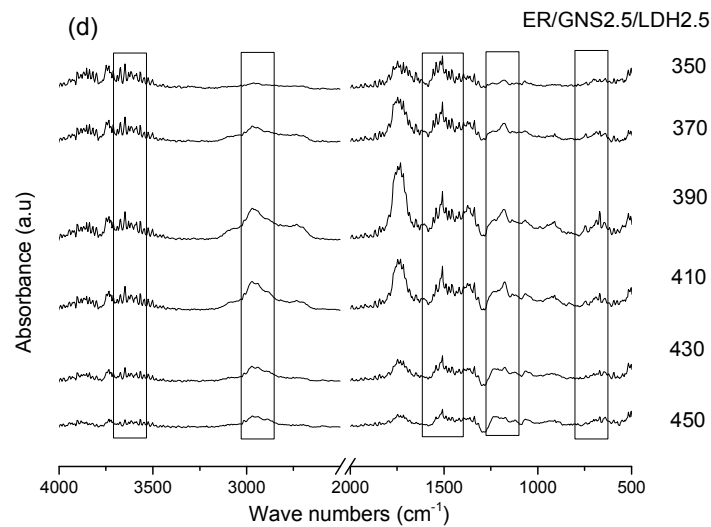
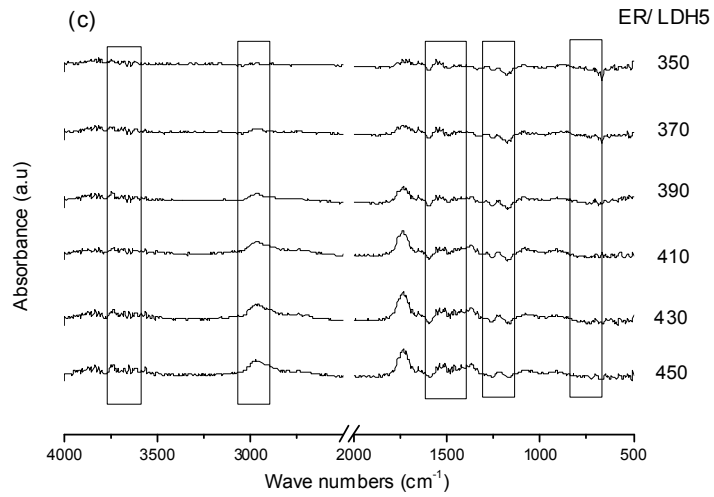
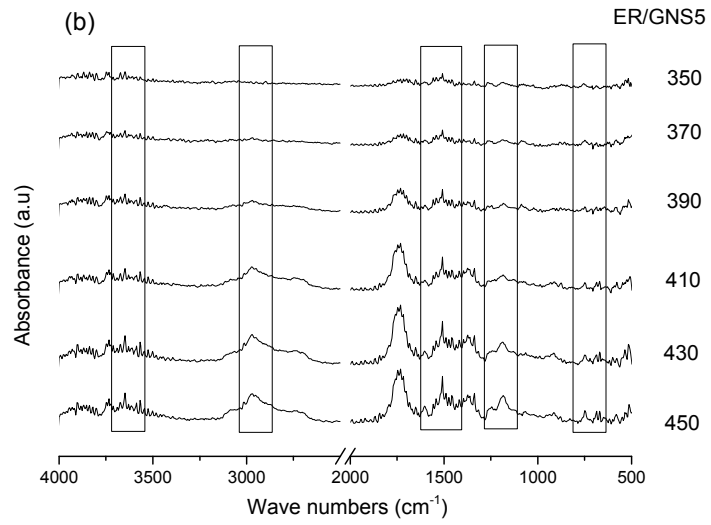
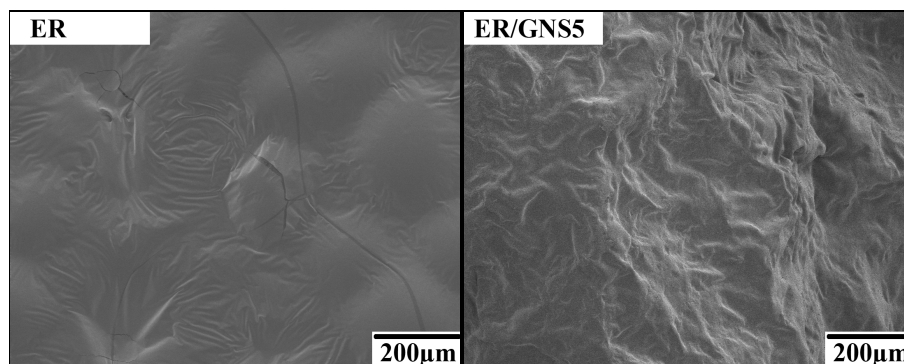


Figure 10. FTIR spectra of gas products for ER, ER/GNS5, ER/LDH5 and ER/GNS2.5/LDH2.5 composites at 350-450°C.

The TG curves and data of ER, ER/GNS5, ER/LDH5 and ER/GNS2.5/LDH2.5 composites under nitrogen atmosphere were shown in Figure 9 and Table 1. The corresponding 2D TG-FTIR spectra of gas products at 350-450°C during thermal degradation were shown in Figure 10.

As shown from Figure 9 and Table 1, the degradation path of ER was changed by GNS within the temperature range of 400°C and 430°C in ER/GNS composite, the char residue of ER was promoted. The char residue of ER also increased with the addition of LDH. GNS and LDH had no synergistic effect on forming char and improving the thermal stability of ER.

As shown Figure 10, within the temperature range of 410°C and 430°C, the gas products of ER were nitro compound (1600 cm^{-1}), epoxide group (1250 cm^{-1} , $640\text{-}850\text{ cm}^{-1}$), aliphatic ether (1173 cm^{-1}) and aromatic ring. Aromatic ring was significantly reduced and aliphatic ether was almost disappeared in ER/GNS5. GNS changed the decomposition pathway of ER and enhanced the thermal stability of ER, which we have discussed in our pervious paper [5]. The LDH can change the path of ER degradation at two stages. At low temperature, the change of degradation corresponded to the loss of interlayer water of LDH. At high temperature, the change of degradation corresponded to the condensation of hydroxyls of the octahedral layer, together with decomposition of the anion NO_3^{2-} . These two stages of decomposition were strongly endothermic [1]. Within the temperature range of 390°C and 450°C, the gas products of ER/LDH5 were the same as ER, except aromatic ring being almost disappeared. The gas products of ER/GNS/LDH were basically the same with ER. The simultaneous addition of GNS and LDH made the original separate effect of GNS or LDH invalid.



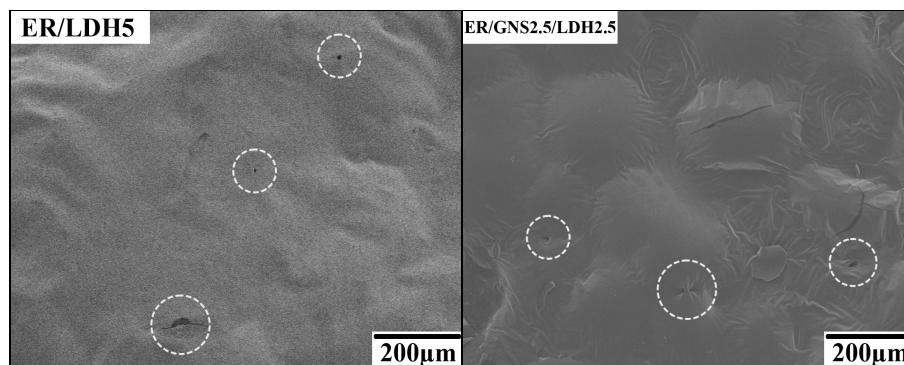
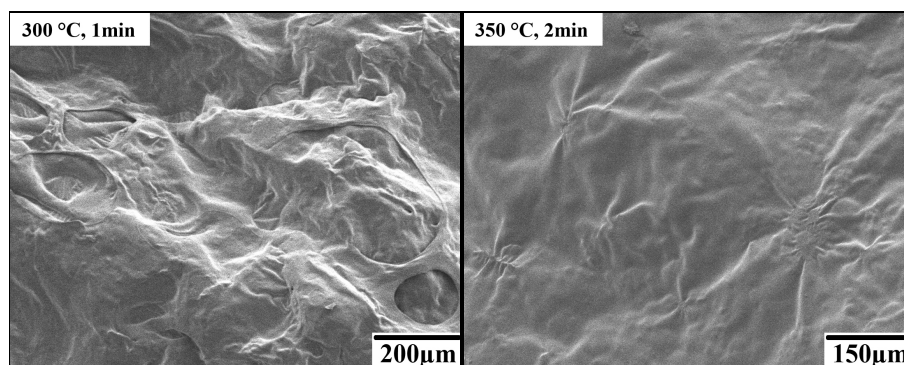


Figure 11. SEM images of the surface char residues of (a) ER, (b) ER/GNS5, (c) ER/LDH5, (d) ER/GNS2.5/LDH2.5 after being calcined.

Figure 11 is SEM images of surface char residues of ER, ER/GNS5, ER/LDH5 and ER/GNS2.5/LDH2.5 composites after being calcined in a muffle furnace. The compactness of surface char residues determines the barrier properties of composites. A slightly rugged surface char residue with some cracks was observed in ER. In ER/GNS5, the residues were slightly folded in deformation. In ER/LDH5, some holes existed in slightly rugged char residue. In ER/GNS2.5/LDH2.5, the morphology of char residues was similar to that in ER, some cracks were observed, which meant the barrier properties were inferior to ER/GNS and ER/LDH. The simultaneous additions of GNS and LDH to ER matrix made the individual effect of GNS or LDH invalid, the compactness of surface char residues of ER/GNS/LDH was not been improved compared to ER/GNS and ER/LDH.



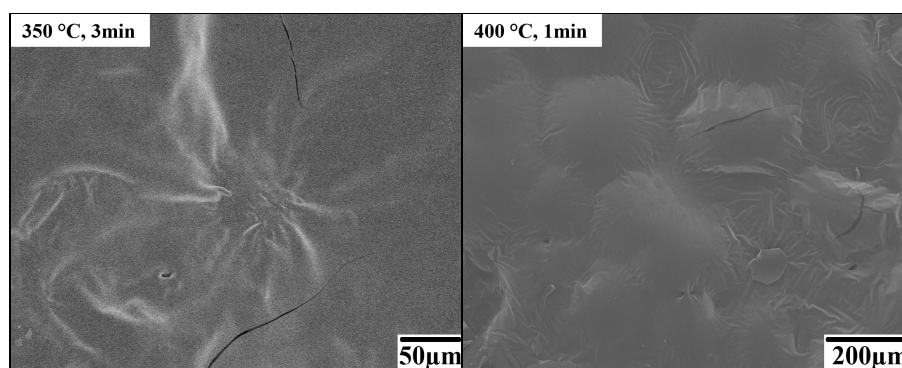


Figure 12. SEM images of the surface char residues of ER/GNS2.5/LDH 2.5 after being calcined in (a) 300°C, 1 min, (b) 350°C, 2 min, (c) 350°C, 3 min, (d) 400°C, 1 min.

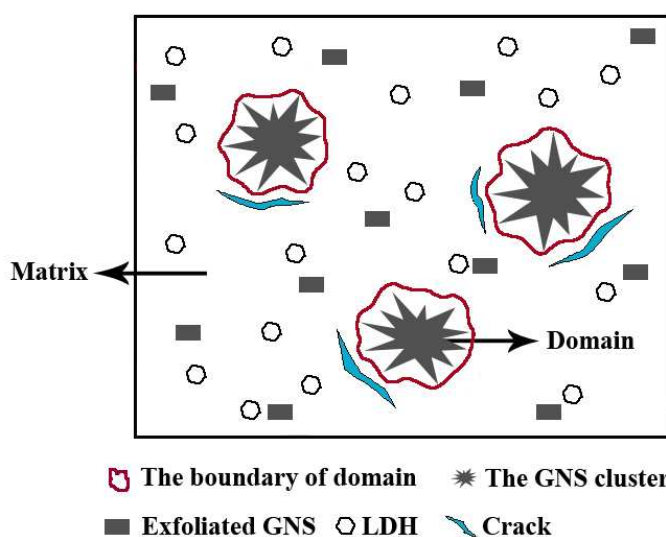


Figure 13. Schematic diagram of char residue formation in ER/GNS/LDH composite.

In order to investigate why the compactness of surface char residue of ER/GNS/LDH was inferior to that of ER/GNS and ER/LDH, the SEM images of the surface char residues of ER/GNS/LDH after being calcined in different temperatures and times were taken. Figure 12 is the SEM images of surface char residues of ER/GNS2.5/LDH2.5 composite after being calcined in a muffle furnace in (a) 300°C, 1 min, (b) 350°C, 2 min, (c) 350°C, 3 min and (d) 400°C, 1 min. Through the morphology changes of surface char, the change of degradation process can be seen and combustion mechanism of ER/GNS/LDH composite can be proposed. When calcined in a muffle furnace in 300°C for 1 min, ER was in semi-molten state, ER segments was moving and the composite was degraded in the heating process. When calcined in 350°C for 2 min, surface char residues was smoothed and the compactness of surface char residues was better. The agglomerated GNS clusters, as shown in TEM image, (Figure 3c), still existed in char residues and formed some sunflower-like structures embedded in the char residues. Another 1

min heating at this temperature, some micro-cracks occurred in char residues at the edge of GNS cluster.

Because the agglomeration of GNS, the system was divided into two parts, which corresponded to the two different combustion mechanisms. Figure 13 shows the schematic diagram of char residue formation in ER/GNS/LDH. From SEM we can see that the char of pure ER have cracks, but the char of ER/GNS and ER/LDH does not have cracks, which means GNS and LDH can inhibit the formation of cracks in ER. In ER/GNS/LDH, the cracks appear again, which means GNS and LDH together cannot inhibit the formation of cracks. From TEM we can see that there are uniform matrix area and domain in ER/GNS/LDH. The uniform matrix area is the mixed region of ER, LDH and exfoliated GNS, while domain is the GNS agglomerations and the ER surrounding. The hexagons and gray rectangles represent the LDH and exfoliated GNS respectively. The red closed loops represent the boundary of domain. The black stars represent the GNS cluster. The light blue stripes are cracks in char residues. Combining with the analysis of Figure 10, we speculate that the cracks in ER/GNS/LDH char are generated by the difference of uniform matrix area and domain. Since the structure of char and the time of char formation are different in these two parts, cracks may occur near the interface of these two parts, which affect the compactness of surface char residues and weaken the barrier effect in ER/GNS/LDH. As a result, there was no synergistic effect of simultaneous additions of GNS and LDH promotes the formation of char and suppressing the gas products of ER/GNS/LDH during combustion. SEM observation and interpretation are also supported by the results in TG and IR tests.

4. Conclusions

In ER/GNS, the exfoliated GNS and agglomerated GNS coexisted. In ER/LDH, all LDH exfoliated. In ER/GNS/LDH, the dispersion of GNS was similar to that in ER/GNS and the dispersion of LDH was similar to that in ER/LDH, with all LDH being exfoliated and GNS being partially exfoliated and partially agglomerated into clusters.

Both GNS and LDH can increase the LOI value of ER. In ER/GNS, the LOI value increased with the increase of GNS content. In ER/GNS/LDH, there was a synergistic effect between GNS and LDH to improve the LOI value of ER. The LOI value was increased from 15.9 to 23.6 by adding 0.5 wt% of GNS and 0.5 wt% of LDH, which was higher than adding 1 wt% of GNS or 1 wt% of LDH alone. The simultaneous additions of GNS and LDH to ER matrix generated additional GNS-LDH interactions, which increased the viscosity of the melt and limited flame propagation through the inhibition of dripping. Furthermore, both GNS and LDH can increase the thermal stability of ER, there was a synergistic effect between GNS and LDH to decrease the THR of ER from 33.4 to 24.6 at the

addition of 2.5 wt% GNS and 2.5 wt% LDH together.

Below the ER onset degradation temperature, GNS didn't decompose, but LDH began to decompose and to release water vapor and carbon dioxide. The GNS can change the path of ER degradation by promoting the char formation. The char residue of ER also increased with the addition of LDH. Because of the agglomeration of some GNS, there are uniform matrix area and domain in ER/GNS/LDH. The uniform matrix area is the mixed region of ER, LDH and exfoliated GNS, while domain is the GNS agglomerations and the ER surrounding. Since the structure of char and the time of char formation were different in these two parts, cracks generated near the interface of these two parts. The compactness of surface char residues and barrier effect of fillers was weakened. As a result, there was no synergistic effect of simultaneous addition of GNS and LDH on promoting the formation of char and suppressing the gas products of ER/GNS/LDH during combustion.

Acknowledgements

Financial support from the National Natural Science Foundation of China (No. 51203137) is acknowledged.

References

- [1] Morgan AB, Wilkie CA. Flame retardant polymer nanocomposites. Hoboken (NJ): John Wiley & Sons; 2007. p. 235–277.
- [2] Becker CM, Gabbardo AD, Wypych F, Amico SC, Composites. 2011; 42: 196–202
- [3] Zaman I, Phan TT, Kuan HC, Meng QS, La LTB, Luong L, Youssf O, Ma J, Polymer. 2011; 52: 1603–1611
- [4] Guo YQ, Bao CL, Song L, Yuan BH, Hu Y, Ind. Eng. Chem. Res. 2011; 50: 7772–7783
- [5] Liu S, Yan HQ, Fang ZP, Wang H, Compos. Sci. Technol. 2014; 90: 40–47
- [6] Kim KS, Jeon IY, Ahn SN, Kwon YD and Baek JB, J. Mater. Chem. 2011; 21: 7337–7342
- [7] Wang X, Hu Y, Song L, Xing WY, Lu HD, Polym. Bull. 2011; 67: 859–873
- [8] Miller SG, Bauer JL, Maryanski MJ, Heimann PJ, Barlowe JP, Gosau JM, Allred RE, Compos. Sci. Technol. 2010; 70: 1120–1125
- [9] Wang X, Hu Y, Song L, Yanga HY, Yu B, Kandola B, Deli D, Thermochimi Acta 2012; 543: 156–164
- [10] Ma HY, Song PA, Fang ZP, Sci. China Chem. 2011; 54: 302–313
- [11] Xiao XC, Xie T, Cheng YT, J. Mater. Chem. 2010; 20: 3508–3514
- [12] Fang M, Zhang Z, Li JF, Zhang HD, Lu HB and Yang YL, J. Mater. Chem. 2010; 20: 9635–9643

- [13] Zhao MQ, Zhang Q, Jia XL, Huang JQ, Zhang YH and Wei F, *Adv. Funct. Mater.* 2010; 20: 677–685
- [14] Zammarano M, Franceschi M, Bellayer S, Gilman JW, Meriani S, *Polymer.* 2005; 46: 9314–9328
- [15] Chan YN, Juang TY, Liao YL, Dai SA, Lin JJ, *Polymer.* 2008; 49: 4796–4801
- [16] Tsai TY, Lu SW, Li FS, *J Phys Chem Solids.* 2008; 69: 1386–1390
- [17] Tseng CH, Hsueh HB, Chen CY, *Compos. Sci. Technol.* 2007; 67: 2350–2362
- [18] Lv SC, Yuan Y, Shi WF, *Prog Org Coat.* 2009; 65: 425–430
- [19] Ramanathan T, Abdala AA, Stankovich S, Dikin DA, Alonso MH, Piner RD, Adamson DH, Schniepp HC, Chen X, Ruoff RS, Nguyen ST, Aksay IA, Prud'homme RK, Brinson LC, *Nature nanotechnology.* 2008; 3: 327–331
- [20] Martin-Gallego M, Bernal M.M, Hernandez M, Verdejo R, Lopez-Manchado M.A, *Eur. Polmy. J.* 2013; 49: 1347–1353
- [21] Jeffrey RP, Daniel RD, Christopher WB, Rodney SR, *Polymer.* 2011; 52: 5–25
- [22] Wang Q, Zhang X, Wang CJ, Zhu JH, Guo ZH, Hare DO, *J. Mater. Chem.* 2012; 22: 19113–19121